

Spectral backscattering properties of marine phytoplankton cultures

Amanda L. Whitmire,^{1,*} W. Scott Pegau,² Lee Karp-Boss,³
Emmanuel Boss,³ and Timothy J. Cowles¹

¹Oregon State University, College of Oceanic & Atmospheric Sciences,
104 COAS Admin. Bldg., Corvallis, OR 97331, USA

²Oil Spill Recovery Institute, P.O. Box 705, Cordova, AK 99574, USA

³University of Maine, School of Marine Sciences, 5706 Aubert Hall, Orono, ME 04473-4032, USA

*Whitmire@coas.oregonstate.edu

Abstract: The backscattering properties of marine phytoplankton, which are assumed to vary widely with differences in size, shape, morphology and internal structure, have been directly measured in the laboratory on a very limited basis. This work presents results from laboratory analysis of the backscattering properties of thirteen phytoplankton species from five major taxa. Optical measurements include portions of the volume scattering function (VSF) and the absorption and attenuation coefficients at nine wavelengths. The VSF was used to obtain the backscattering coefficient for each species, and we focus on intra- and interspecific variability in spectral backscattering in this work. Ancillary measurements included chlorophyll-*a* concentration, cell concentration, and cell size, shape and morphology via microscopy for each culture. We found that the spectral backscattering properties of phytoplankton deviate from theory at wavelengths where pigment absorption is significant. We were unable to detect an effect of cell size on the spectral shape of backscattering, but we did find a relationship between cell size and both the backscattering ratio and backscattering cross-section. While particulate backscattering at 555 nm was well correlated to chlorophyll-*a* concentration for any given species, the relationship was highly variable between species. Results from this work indicate that phytoplankton cells may backscatter light at significantly higher efficiencies than what is predicted by Mie theory, which has important implications for closing the underwater and remotely sensed light budget.

© 2010 Optical Society of America

OCIS codes: (010.1350) Backscattering; (290.5850) Scattering, particles; (000.1430) Biology and medicine

References and links

1. H. R. Gordon, O. B. Brown, and M. M. Jacobs, "Computed relationships between the inherent and apparent optical properties of a flat homogeneous ocean," *Appl. Opt.* **14**(2), 417–427 (1975).
2. C. D. Mobley, *Light and Water: Radiative Transfer in Natural Waters* (Academic, 1994).
3. T. Dickey, M. Lewis, and G. Chang, "Optical oceanography: Recent advances and future directions using global remote sensing and in situ observations," *Rev. Geophys.* **44**(1), RG1001 (2006), doi:10.1029/2003RG000148.
4. D. Stramski, E. Boss, D. Bogucki, and K. J. Voss, "The role of seawater constituents in light backscattering in the ocean," *Prog. Oceanogr.* **61**(1), 27–56 (2004).
5. R. A. Meyer, "Light scattering from biological cells: dependence of backscatter radiation on membrane thickness and refractive index," *Appl. Opt.* **18**(5), 585–588 (1979).
6. M. S. Quinby-Hunt, A. J. Hunt, K. Loffitus, and D. Shapiro, "Polarized-light scattering studies of marine Chlorella," *Limnol. Oceanogr.* **34**(8), 1587–1600 (1989).
7. J. C. Kitchen, and J. R. V. Zaneveld, "A three-layered sphere model of the optical properties of phytoplankton," *Limnol. Oceanogr.* **37**(8), 1680–1690 (1992).
8. A. Quirantes, and S. Bernard, "Light scattering by marine algae: two-layer spherical and nonspherical models," *J. Quant. Spectrosc. Radiat. Transf.* **89**(1-4), 311–321 (2004).

9. W. R. Clavano, E. Boss, and L. Karp-Boss, "Inherent Optical Properties of Non-Spherical Marine-Like Particles - From Theory to Observations," *Oceanography and Marine Biology: An Annual Review* **45**, 1–38 (2007).
10. A. Morel, and A. Bricaud, "Theoretical results concerning light absorption in a discrete medium, and application to specific absorption of phytoplankton," *Deep-Sea Res.* **28**(11), 1375–1393 (1981).
11. A. Bricaud, A. Morel, and L. Prieur, "Optical efficiency factors of some phytoplankters," *Limnol. Oceanogr.* **28**(5), 816–832 (1983).
12. A. Bricaud, and A. Morel, "Light attenuation and scattering by phytoplanktonic cells: a theoretical modeling," *Appl. Opt.* **25**(4), 571–580 (1986).
13. A. Morel, and A. Bricaud, "Inherent optical properties of algal cells, including picoplankton. Theoretical and experimental results," *Can. Bull. Fish. Aquat. Sci.* **214**, 521–559 (1986).
14. A. Morel, and Y.-H. Ahn, "Optical efficiency factors of free-living marine bacteria: Influence of bacterioplankton upon the optical properties and particulate organic carbon in oceanic waters," *J. Mar. Res.* **48**(1), 145–175 (1990).
15. A. Morel, and Y.-H. Ahn, "Optics of heterotrophic nanoflagellates and ciliates: A tentative assessment of their scattering role in oceanic waters compared to those of bacterial and algal cells," *J. Mar. Res.* **49**(1), 177–202 (1991).
16. D. Stramski, and D. A. Kiefer, "Light scattering by microorganisms in the open ocean," *Prog. Oceanogr.* **28**(4), 343–383 (1991).
17. Y.-H. Ahn, A. Bricaud, and A. Morel, "Light backscattering efficiency and related properties of some phytoplankters," *Deep-Sea Res.* **39**(11–12), 1835–1855 (1992).
18. D. Stramski, and C. D. Mobley, "Effects of microbial particles on oceanic optics: A database of single-particle optical properties," *Limnol. Oceanogr.* **42**(3), 538–549 (1997).
19. D. Stramski, A. Bricaud, and A. Morel, "Modeling the inherent optical properties of the ocean based on the detailed composition of the planktonic community," *Appl. Opt.* **40**(18), 2929–2945 (2001).
20. H. Volten, J. F. Haan, J. W. Hovenier, R. Schreurs, W. Vassen, A. G. Dekker, H. J. Hoogenboom, F. Charlton, and R. Wouts, "Laboratory Measurements of Angular Distributions of Light Scattered by Phytoplankton and Silt," *Limnol. Oceanogr.* **43**(6), 1180–1197 (1998).
21. R. D. Vaillancourt, C. W. Brown, R. R. L. Guillard, and W. M. Balch, "Light backscattering properties of marine phytoplankton: relationships to cell size, chemical composition, and taxonomy," *J. Plankton Res.* **26**(2), 191–212 (2004).
22. C. S. Yentsch, and D. W. Menzel, "A method for the determination of phytoplankton chlorophyll and phaeophytin by fluorescence," *Deep-Sea Res.* **10**, 221–231 (1963).
23. W. S. Pegau, D. Gray, and J. R. V. Zaneveld, "Absorption and attenuation of visible and near-infrared light in water: dependence on temperature and salinity," *Appl. Opt.* **36**(24), 6035–6046 (1997).
24. J. R. V. Zaneveld, J. C. Kitchen, and C. C. Moore, "Scattering error correction of reflecting tube absorption meter," *Ocean Optics XII*, Proc. SPIE **2258**, 44–55 (1994).
25. R. A. Maffione, and D. R. Dana, "Instruments and methods for measuring the backward-scattering coefficient of ocean waters," *Appl. Opt.* **36**(24), 6057–6067 (1997).
26. E. Boss, and W. S. Pegau, "Relationship of light scattering at an angle in the backward direction to the backscattering coefficient," *Appl. Opt.* **40**(30), 5503–5507 (2001).
27. H. Buiteveld, J. H. M. Hakvoort, and M. Donze, "Optical properties of pure water," *Ocean Optics XII*, Proc. SPIE **2258** (1994).
28. T. Oishi, "Significant relationship between the backward scattering coefficient of sea water and the scatterance at 120°," *Appl. Opt.* **29**(31), 4658–4665 (1990).
29. M. S. Twardowski, H. Claustre, S. A. Freeman, D. Stramski, and Y. Huot, "Optical backscattering properties of the "clearest" natural waters," *Biogeosci.* **4**(6), 1041–1058 (2007), www.biogeosciences.net/4/1041/2007.
30. E. Boss, W. S. Pegau, M. Lee, M. S. Twardowski, E. Shybanov, G. Korotaev, and F. Baratange, "The particulate backscattering ratio at LEO-15 and its use to study particle composition and distribution," *J. Geophys. Res.* **109**(C1), C01014 (2004), doi:10.1029/2002JC001514.
31. J. J. Walsh, J. K. Jolliff, B. P. Darrow, J. M. Lenos, S. P. Milroy, A. Remsen, D. A. Dieterle, K. L. Carder, F. R. Chen, G. A. Vargo, R. H. Weisberg, K. A. Fanning, F. E. Muller-Karger, E. Shinn, K. A. Steidinger, C. A. Heil, C. R. Tomas, J. S. Prospero, T. N. Lee, G. J. Kirkpatrick, T. E. Whitley, D. A. Stockwell, T. A. Villareal, A. E. Jochens, and P. S. Bontempi, "Red tides in the Gulf of Mexico: Where, when, and why?" *J. Geophys. Res.* **111**(C11 C11003), 1–46 (2006).
32. J.-F. Berthon, E. Shybanov, M. E.-G. Lee, and G. Zibordi, "Measurements and modeling of the volume scattering function in the coastal northern Adriatic Sea," *Appl. Opt.* **46**(22), 5189–5203 (2007).
33. D. Stramski, M. Babin, and S. B. Woźniak, "Variations in the optical properties of terrigenous mineral-rich particulate matter suspended in seawater," *Limnol. Oceanogr.* **52**, 2418–2433 (2007).
34. J. M. Sullivan, and M. S. Twardowski, "Angular shape of the oceanic particulate volume scattering function in the backward direction," *Appl. Opt.* **48**(35), 6811–6819 (2009).
35. T. J. Petzold, "Volume scattering functions for selected ocean waters," Contract No. N62269–71-C-0676, UCSD, SIO Ref. 72–78 (1972).
36. C. Moore, M. S. Twardowski, and J. R. V. Zaneveld, "The ECO-VSF: a multiangle scattering sensor for determination of the volume scattering function in the backward direction," presented at Ocean Optics XV, Monaco (2000).

37. J. M. Sullivan, M. S. Twardowski, P. L. Donaghay, and S. A. Freeman, "Use of optical scattering to discriminate particle types in coastal waters," *Appl. Opt.* **44**(9), 1667–1680 (2005).
38. J. Prentice, A. D. Weidemann, W. S. Pegau, K. J. Voss, M. Lee, E. Shybanov, O. Martynov, A. Laux, A. L. Briggs, and G. Chang, "Laboratory comparisons of optical scattering instrumentation," *Ocean Optics XVI*, Santa Fe, NM (2002).
39. M. E. Lee, and M. R. Lewis, "A new method for the measurement of the optical volume scattering function in the upper ocean," *J. Atmos. Ocean. Technol.* **20**(4), 563–671 (2003).
40. A. Bricaud, A. L. Bedhomme, and A. Morel, "Optical properties of diverse phytoplanktonic species: Experimental results and theoretical interpretation," *J. Plankton Res.* **10**(5), 851–873 (1988).
41. E. Boss, R. Collier, G. Larson, K. Fennel, and W. S. Pegau, "Measurements of spectral optical properties and their relation to biogeochemical variables and processes in Crater Lake, Crater Lake National Park, OR," *Hydrobiologia* **574**(1), 149–159 (2007).
42. A. L. Whitmire, E. Boss, T. J. Cowles, and W. S. Pegau, "Spectral variability of the particulate backscattering ratio," *Opt. Express* **15**(11), 7019–7031 (2007).
43. G. Dall'Olmo, T. K. Westberry, M. J. Behrenfeld, E. Boss, and W. H. Slade, "Significant contribution of large particles to optical backscattering in the open ocean," *Biogeosci.* **6**(6), 947–967 (2009).
44. A. Morel, "The scattering of light by seawater, experimental results and theoretical approach," (translated from French), in *AGARD Lect. Ser.*, pp. 3.1.1.-3.1.76 (1973).
45. C. F. Bohren, and D. R. Huffman, *Absorption and Scattering of Light by Small Particles* (John Wiley & Sons, 1983).
46. H. Loisel, and D. Stramski, "Estimation of the inherent optical properties of natural waters from the irradiance attenuation coefficient and reflectance in the presence of Raman scattering," *Appl. Opt.* **39**(18), 3001–3011 (2000).
47. E. Aas, "Refractive index of phytoplankton derived from its metabolite composition," *J. Plankton Res.* **18**(12), 2223–2249 (1996).
48. Y. Huot, A. Morel, M. S. Twardowski, D. Stramski, and R. A. Reynolds, "Particle optical backscattering along a chlorophyll gradient in the upper layer of the eastern South Pacific Ocean," *Biogeosci.* **5**(2), 495–507 (2008).
49. R. F. Davis, C. C. Moore, J. R. V. Zaneveld, and J. M. Napp, "Reducing the effects of fouling on chlorophyll estimates derived from long-term deployments of optical instruments," *J. Geophys. Res.* **102**(C3), 5851–5855 (1997).
50. A. L. Whitmire, "The spectral backscattering properties of marine particles," Ph.D. dissertation, Oregon State University, 2008. ScholarsArchive@OSU, 28 Oct. 2008 <<http://hdl.handle.net/1957/9088>>.
51. K. Witkowski, T. Krol, A. Zielinski, and E. Kuten, "A light-scattering matrix for unicellular marine phytoplankton," *Limnol. Oceanogr.* **43**(5), 859–869 (1998).
52. L. E. Graham, and L. W. Wilcox, *Algae* (Prentice Hall, 2000).
53. Y. Bhaud, D. Guillebault, J. Lennon, H. Defacque, M. O. Soyer-Gobillard, and H. Moreau, "Morphology and behaviour of dinoflagellate chromosomes during the cell cycle and mitosis," *J. Cell Sci.* **113**(Pt 7), 1231–1239 (2000).
54. A. Samoc, A. Miniewicz, M. Samoc, and J. G. Grote, "Refractive-index anisotropy and optical dispersion in films of deoxyribonucleic acid," *J. Appl. Polym. Sci.* **105**(1), 236–245 (2007).
55. M. A. Faust, "Structure of the periplast of *Cryptomonas ovata* var. *palustris*," *J. Phycol.* **10**, 121–124 (1974).
56. U. J. Santore, "Some aspects of taxonomy in the Cryptophyceae," *New Phytol.* **98**(4), 627–646 (1984).
57. D. Stramski, and J. Piskozub, "Estimation of scattering error in spectrophotometric measurements of light absorption by aquatic particles from three-dimensional radiative transfer simulations," *Appl. Opt.* **42**(18), 3634–3646 (2003).
58. G. A. Jackson, R. Maffione, D. K. Costello, A. L. Alldredge, B. E. Logan, and H. G. Dam, "Particle size spectra between 1 μ m and 1 cm at Monterey Bay determined using multiple instruments," *Deep-Sea Res.* **44**(11), 1739–1767 (1997), doi:10.1016/S0967-0637(97)00029-0.

1. Introduction

The structure and function of marine ecosystems are largely dictated by the composition of the phytoplankton community. Likewise, the bulk inherent optical properties of the ocean (absorption and angular scattering) are determined by the sum of those of its constituents (water, particles, and dissolved substances) [1,2]. Historical methods of monitoring phytoplankton abundance and distribution generally treat the community in bulk, due mainly to an inability to effectively and efficiently isolate and monitor specific phytoplankton taxa. Optical instruments are now being used on a variety of platforms at time and space scales relevant to phytoplankton physiology and ecology [3]. However, our understanding of how diverse phytoplankton taxa contribute to bulk optical measurements remains limited. This is especially true of the backscattering properties of marine phytoplankton, due to a paucity of measurements of this parameter on laboratory cultures [4]. A comprehensive understanding of

how marine phytoplankton contribute to the bulk backscattering signal in the ocean is critical for accurate interpretation of remote sensing data because the ocean reflectance is determined by the ratio of backscattering to absorption [1]. Conversely, the development of inversions of ocean color to retrieve the concentration and type of the underlying particles strongly relies upon information about the factors influencing the backscattering coefficient and spectrum in the ocean.

Historically, the backscattering properties of phytoplankton cells were investigated through the use of theoretical models because the instrumentation required to measure backward scattering was not commercially available. Early work that employed scattering theory for coated spheres (i.e., representing a cell as having a cell membrane or cell wall and a homogeneous interior) indicated that it was essential to account for a cell membrane when using models to represent biological cells because models that assumed homogeneous spheres (no cell wall or cell membrane) underestimated backward scattering [5]. Likewise, several modeling studies that incorporated layered or coated spheres [6–8] or non-spherical particles [8,9] also concluded that assuming sphericity and homogeneity resulted in underestimates of the backscattering coefficient by up to an order of magnitude.

Despite these findings, a majority of the studies that use models to obtain backscattering by phytoplankton and other marine microbial cells rely upon Mie's theory of scattering by an homogeneous sphere to model light absorption and scattering [10–19]. These studies concluded that backscattering by phytoplankton, marine bacteria, ciliates and/or flagellates was weak compared to other marine particles such as detritus or lithogenic materials. The supposition that phytoplankton cells are weak backscatterers has strong ramifications in how they are modeled as a portion of the diverse oceanic particle population in radiative transfer simulations and remote sensing applications.

The backscattering properties of marine phytoplankton have only recently been rigorously measured in the laboratory on a limited basis [20,21]. Volten et al. [20] made detailed measurements of the volume scattering function for several phytoplankton species at a single wavelength, 633 nm. They found that morphology influenced the scattering distribution, but not in ways that were predictable. For example, two species with a similar shape produced different scattering signals, while two cultures with very different shapes, a cylinder and a sphere, produced similar angular scattering patterns. Volten et al. [20] also found that internal structures, like gas vacuoles, had a significant impact on the scattering distribution. In comparing their measurements with Mie model simulations of the phytoplankton cells in their study, Volten et al. [20] concluded that the Mie model, with its assumptions of sphericity and homogeneity, did not produce good approximations of scattering by phytoplankton. Vaillancourt et al. [21] also found that the Mie model was unable to reproduce the magnitude of backscattering that they observed for phytoplankton cultures when "typical phytoplankton" values of the real refractive index, n , were used as inputs to the model ($n = 1.06 - 1.08$).

An analysis of the spectral backscattering properties of marine phytoplankton cultures at four wavelengths did not find any significant spectral variation between cultures [21]. The spectral backscattering coefficients for all of the cultures studied in Vaillancourt et al. [21] were normalized to cell concentration to obtain backscattering efficiencies. Relationships between backscattering efficiency and chlorophyll-*a*, particulate organic carbon, and cell size were all analyzed at a single wavelength. Measurements of complementary inherent optical properties, the absorption, attenuation, and scattering coefficients, were not collected in this study, which makes it difficult to place the backscattering measurements into context and compare them with the optical properties of other important marine particle types.

The shortage of direct measurements of the spectral backscattering properties of marine phytoplankton and the discrepant results of various modeling studies highlight the need for additional empirical studies on this topic. This work presents results from laboratory analysis of the backscattering properties of thirteen phytoplankton species from five major taxa (diatoms, dinoflagellates, chlorophytes, cryptophytes, and prymnesiophytes; fifteen strains

total). Optical measurements included portions of the volume scattering function (VSF) at six wavelengths, total (minus water) absorption and attenuation at nine wavelengths, and stimulated fluorescence. The VSF was used to obtain the backscattering coefficient for each species, and we focused on intra- and interspecific variability in spectral backscattering in this work. We also investigated the spectral and angular variability in the conversion factor for single-angle VSF measurements to the backscattering coefficient for phytoplankton cultures, which may be applicable to in situ monoculture blooms and harmful algal bloom events. Ancillary measurements include chlorophyll-*a* concentration and cell size, shape and morphology via Coulter counter and/or light microscopy. The goal of this work is to elucidate how and to what extent the diversity in size, shape, and morphology contributes to variability in backscattering of phytoplankton within and between taxa.

2. Methods

2.1 Phytoplankton cultures

Table 1. Summary of phytoplankton characteristics. Optical data are shown at 442 nm

| Culture | Strain | Algal Class | Shape | ESD [μm] | $b^*_{\text{bp}} \times 10^3$ |
|---|--------|---------------------|---|------------------------------------|-------------------------------|
| <i>Ceratium longipes</i> ⁻ | 1170 | Dinophyceae |  | 160 ⁺ , 55 ⁻ | 9.797 |
| <i>Chlorella sp.</i> [#] | n/a | Trebouxiophyceae |  | 4.13 | 23.598 |
| <i>Coscinodiscus radiatus</i> ⁻ | 312 | Coscinodiscophyceae |  | 94.06* | 10.970 |
| <i>Coscinodiscus radiatus</i> ⁻ | 310 | Coscinodiscophyceae |  | 33.48 | 463.812 |
| <i>Cryptomonas profunda</i> [#] | n/a | Cryptophyceae |  | 9.08 | 1.038 |
| <i>Ditylum brightwellii</i> ⁻ | 2227 | Coscinodiscophyceae |  | 61 ⁺ , 52 ⁺ | 0.341 |
| <i>Dunaliella tertiolecta</i> [#] | n/a | Chlorophyceae |  | 6.88 | 1.083 |
| <i>Gymnodinium simplex</i> ⁻ | 419 | Dinophyceae |  | 11.69 | 9.194 |
| <i>Heterocapsa triquetra</i> ⁻ | 440 | Dinophyceae |  | 13.33 | 5.786 |
| <i>Isochrysis galbana</i> ⁻ | 1323 | Prymnesiophyceae |  | 3.9 | 9.982 |
| <i>Phaeodactylum tricorutum</i> [#] | n/a | Bacillariophyceae |  | 4.14 | 2.358 |
| <i>Thalassiosira pseudonana</i> [^] | 709 | Coscinodiscophyceae |  | 4.2 | 1.898 |
| <i>Thalassiosira pseudonana</i> ⁻ | 1010 | Coscinodiscophyceae |  | 13.93 | 0.526 |
| <i>Thalassiosira rotula</i> ⁻ | 1018 | Coscinodiscophyceae |  | 16.65 | 10.258 |
| <i>Thalassiosira weissflogii</i> [#] | n/a | Coscinodiscophyceae |  | 10.64 | 2.924 |

| | $b_{\text{bp}}/b_{\text{p}}$ | σ_{bb} | Q_{a} | Q_{b} | Q_{c} | Q_{bb} |
|--|------------------------------|------------------------|----------------|----------------|----------------|-----------------|
| <i>Ceratium longipes</i> ⁻ | 0.0264 | 1.23x10 ⁻⁰⁹ | 0.617 | 2.325 | 2.942 | 0.061 |
| <i>Chlorella sp.</i> [#] | 0.0079 | 1.67x10 ⁻¹³ | 0.409 | 1.585 | 1.994 | 0.012 |
| <i>Coscinodiscus radiatus</i> (312) ⁻ | 0.0290 | 4.02x10 ⁻¹⁰ | 0.688 | 2.409 | 3.096 | 0.058 |
| <i>Coscinodiscus radiatus</i> (310) ⁻ | 0.0240 | 2.35x10 ⁻¹⁰ | 3.302 | 9.218 | 12.521 | 0.267 |
| <i>Cryptomonas profunda</i> [#] | 0.0131 | 1.78x10 ⁻¹² | 0.970 | 2.068 | 3.037 | 0.027 |
| <i>Ditylum brightwellii</i> ⁻ | 0.0116 | 1.75x10 ⁻¹¹ | 0.244 | 0.511 | 0.755 | 0.006 |
| <i>Dunaliella tertiolecta</i> [#] | 0.0061 | 4.81x10 ⁻¹³ | 0.982 | 2.131 | 3.113 | 0.013 |
| <i>Gymnodinium simplex</i> ⁻ | 0.0210 | 1.93x10 ⁻¹¹ | 2.396 | 8.545 | 10.942 | 0.180 |
| <i>Heterocapsa triquetra</i> ⁻ | 0.0195 | 7.56x10 ⁻¹² | 1.218 | 2.772 | 3.990 | 0.054 |
| <i>Isochrysis galbana</i> ⁻ | 0.0047 | 1.31x10 ⁻¹³ | 0.601 | 2.312 | 2.913 | 0.011 |
| <i>Phaeodactylum</i> <i>tricorutum</i> [#] | 0.0035 | 8.60x10 ⁻¹⁴ | 0.650 | 1.826 | 2.476 | 0.006 |
| <i>Thalassiosira pseudonana</i> [^] | 0.0055 | 1.49x10 ⁻¹³ | 0.591 | 1.949 | 2.541 | 0.011 |
| <i>Thalassiosira pseudonana</i> ⁻ | 0.0096 | 1.95x10 ⁻¹² | 0.973 | 1.336 | 2.310 | 0.013 |
| <i>Thalassiosira rotula</i> ⁻ | 0.0246 | 1.53x10 ⁻¹¹ | 1.246 | 2.864 | 4.110 | 0.070 |
| <i>Thalassiosira weissflogii</i> [#] | 0.0105 | 1.16x10 ⁻¹² | 0.662 | 1.245 | 1.910 | 0.013 |

ESD is equivalent spherical diameter from Coulter counter measurements (Gaussian fit to data), except where size was determined via microscopy (denoted by *).

⁻CCMP; [^]CCCM; [#]Source unknown; ⁺Size includes spines; ⁻Size excludes spines

Most cultures were obtained from the Provasoli-Guillard Center for Culture of Marine Phytoplankton (CCMP) and the Canadian Center for the Cultivation of Microorganisms (CCCM; see Table 1). The species used in this experiment were selected to reflect the diversity of cell sizes and morphologies observed in phytoplankton and include representatives from four taxonomic groups: diatoms (centric (with and without spines) and pennate), dinoflagellates (armored and unarmored), chlorophytes, and prymnesiophytes (see Table 1 for information regarding the species). Although some of the diatom species chosen for this study can form chains, in our cultures they were all unicellular. All were grown in L1-enriched seawater media that was autoclaved and then filter sterilized using a 0.22 μm filter (Millipore, Steritop). Cultures were incubated at 17°C with an illumination of approximately 100 $\mu\text{mol photons m}^{-2} \text{ s}^{-1}$ under a 14:10 dark:light cycle. Cells were maintained in exponential growth by diluting them as needed with fresh media. The rate of dilution varied between species, depending on their growth rate determined daily via *in vivo* fluorometry. These cultures were not axenic, but we believe that bacterial contamination was very low to negligible in most cultures. We discuss our approach for assessing the possible influence of non-algal particles in Section 4.4.

2.2 Optical measurements

Measurements of the volume scattering function (VSF) were conducted in a custom 12½ inch (inner dimension) plexi-glass box that was built to replicate the manufacturer's standard calibration chamber (HOBI Labs, Inc.). To check for reflections in the tank or sensitivity to instrument orientation, we filled the chamber with deionized water (DIW), rotated the HS6 in the chamber, and collected measurements in various orientations. None of the data from varying orientations were statistically different, which indicated that no reflected light reached the detectors. We also performed dilution series tests with liquid antacid (fine chalk suspension; Mylanta) and polystyrene beads. Tank effects would have manifested as a non-linear sensor response in the dilution series', but we found none. Nevertheless, the same instrument orientation was used in each experiment to eliminate possible handling error. The chamber was filled with approximately 25 liters of 0.2 μm -filtered seawater (FSW) and a Hydrosat-6 (HS6) was suspended with the instrument face one inch below the surface. The box was covered in opaque black cloth to exclude ambient light during measurements. An ac-9 (WET Labs, Inc.) was attached in-line with the calibration chamber and sample medium was circulated through the system with a small pump (Sea-Bird SBE-5P). After collecting a filtered seawater measurement sequentially with each instrument, 500 mL of culture was added to the sample chamber. The culture suspension was gently but thoroughly mixed again, and measurements were taken immediately. Sequential additions of culture were made until the entire culture volume had been added, generally between two and two and a half liters total. After each round of optical measurements was complete, aliquots of FSW and then culture suspension were collected for chlorophyll, Coulter counter, and microscopic analysis. Experiments were conducted as close to noon as possible each day so that cultures would be in the same phase of their diel cycle for each experiment. The sample box was thoroughly rinsed with DIW between experiments. Measurements of DIW were taken daily to check for sensor drift or chamber fouling. The DIW measurements were not used in data processing or correction for the HS6.

2.3 Ancillary measurements

Coulter counter measurements were conducted on the FSW media and on each addition of culture immediately following each experiment. We used a 100 μm aperture with a one milliliter sample volume. This provided a reliable particle size distribution and concentration range from 2 to 60 microns in equivalent spherical diameter (ESD). Removing the FSW counts from the cultures had a negligible impact on particle size distributions and particle counts, so we did not remove this 'blank' from the Coulter measurements. The mean size of a

culture (ESD) was determined by fitting a Gaussian function to the Coulter counter frequency distribution (raw particle counts normalized to each bin width, in log space). Cell concentration was estimated by summing all of the raw particle counts within two standard deviations of the mean particle size determined by the Gaussian fit. When cells were too large for the Coulter counter (*Ceratium longipes*, e.g.), cell dimensions and concentration were obtained from preserved samples via light microscopy, and mean values were used to calculate a cross-sectional area for each culture. Comparisons between ESD estimates from the Coulter counter agreed well with the sizes based on microscopy. Chlorophyll-*a* measurements were collected using a standard extraction technique [22].

2.4 Instruments & data processing

Absorption and attenuation were measured at nine wavelengths with a WET Labs ac-9 (412, 442, 488, 510, 532, 555, 650, 676, and 715 nm). DIW measurements were collected daily for calibrations. DIW data were temperature corrected and then subtracted from raw FSW and culture measurements. The data were then corrected for temperature and salinity [23], and the absorption coefficient was corrected for scattering using the proportional method [24]. This scattering correction assumes that the volume scattering function (VSF or β) is independent of wavelength. Indeed, measurements of the volume scattering function for thirteen other phytoplankton cultures (see Section 2.5 below) did not show any significant spectral variability (data not shown). The mean value of the absorption, scattering, and attenuation coefficients were calculated at each wavelength to obtain a single parameter value for each culture at each dilution step.

The VSF was measured at 140 degrees (centroid angle with 25 degree full-width half-max, FWHM) and six wavelengths (442, 488, 532, 555, 620, and 676 nm; 10 nm FWHM) with the HOBI Labs Hydrosat-6 (HS6) instrument [25]. We performed regular calibrations of the instrument using a manufacturer-supplied calibration chamber and Spectralon target. We did not use the processing software provided with the instrument; instead, all processing was accomplished with our own routines via Matlab. We obtained raw values of β from the HS6 and corrected for attenuation along the path length of the instrument using data obtained with an ac-9 (the “ σ -correction”; [25]). We then removed pure water volume scattering, β_w , from the sample volume scattering function, β , to obtain β_p , the volume scattering function due to phytoplankton and other suspended particles associated with the culture [26]. We used estimates for pure seawater volume scattering from Buiteveld et al. [27]. These β_p values were then converted to the backscattering coefficient using a conversion coefficient, χ_p (see Section 2.5). Derived parameters for the HS6 include volume scattering by particles at 140 degrees, and the total and particulate backscattering coefficients ($b_b(\lambda)$ and $b_{bp}(\lambda)$ respectively). To account for any possible tank or filtered media effects, we subtracted $b_{bp}(\lambda)$ for FSW from $b_{bp}(\lambda)$ for each culture suspension.

2.5 Angular and spectral variation in the conversion factor, χ_p , for phytoplankton cultures

Mie theory shows that for angles near 120 degrees the ratio of the VSF at 120 degrees to backscattering for particles does not vary significantly between a wide range in particle properties and sizes [29]. This theoretical relationship facilitates the use of a single-angle scattering meter to estimate the backscattering coefficient. Empirical data continue to demonstrate that measuring scattering at one backward angle is a robust approach to estimating the backscattering coefficient in oceanic waters [29–34]. However, there is some uncertainty concerning the variability in the VSF for phytoplankton, and whether the use of the conversion factor, χ_p , can be applied to derive the backscattering coefficient from a single-angle measurement for phytoplankton cultures [31].

There are presently three approaches for the estimation of the backscattering coefficient from volume scattering measurements. By definition, the backscattering coefficient is the integral of the VSF over the backward hemisphere:

$$b_b = 2\pi \int_{\pi/2}^{\pi} \beta(\theta) \sin \theta d\theta \quad (1)$$

This approach is rarely used because it requires detailed scattering information over a wide angular range, and instrumentation is not yet commercially available to carry out such a measurement (though various prototype in situ instruments have been used on a limited basis for several decades, e.g [35].). An alternative method was developed by Moore et al. [36] and refined by Sullivan et al. [37]. This approach uses scattering measurements at three angles in the backward direction (100, 125, and 150 degrees), and a fourth value for scattering flux at 180 degrees ($2\pi\sin\theta = 0$). A third-order polynomial is then fit to scattering flux at these four angles, and is integrated from $\pi/2$ to π to estimate $b_b(\lambda)$. A third method for estimating the backscattering coefficient is to measure scattering at one backward angle and convert it to $b_b(\lambda)$ using a theoretically or empirically derived conversion factor [25,28]. We used this approach because at the time of our sampling, the Hydrosat-6, which measures the VSF at a single angle, was the only commercially available backscattering sensor with multiple wavelengths.

Using this approach, volume scattering is converted to the backscattering coefficient in the following manner:

$$b_{bp}(\lambda) = 2\pi\chi_p(\theta)\beta_p(\lambda, \theta) \quad (2)$$

where β_p is the particulate VSF at a given wavelength (λ) and scattering angle (θ), and χ_p is a conversion factor to account for the relationship between scattering at one angle and the integral of the VSF from 90 to 180 degrees. χ_p varies with angle as a function of the shape (or slope) of the particle size distribution in the sampling volume, and the real and imaginary refractive index of the bulk particle population [28].

While earlier studies found no spectral dependence in χ_p for oceanic particles [26] or phytoplankton monocultures [21], Chami et al. [31] recently showed significant spectral variation in χ_p for phytoplankton cultures at 140 degrees. As described earlier, our laboratory measurements of β were obtained with a Hydrosat-6 instrument at the single scattering angle of 140 degrees. It was therefore necessary to address these conflicting results before proceeding with our analyses.

To address this issue, we made use of results obtained at a community ‘scattering workshop’ (<http://www.opl.ucsb.edu/ScatteringWorkshop> [38];). During the workshop, a newly developed multi-spectral volume scattering meter (VSM) was tested alongside several other scattering sensors for measurements of polystyrene beads, Maalox solution, local river water, and several phytoplankton monocultures. We used the VSM data to examine the variability in the conversion factor, $\chi_p(\lambda, \theta)$, for thirteen phytoplankton cultures at 6 wavelengths (443, 490, 510, 555, 590, and 620 nm). While the exact species of phytoplankton cultures sampled did not match perfectly between our study and the workshop (five were the same), both studies examined representatives of the same taxonomic groups: diatoms, dinoflagellates and flagellates. This prototype VSM was the same type of instrument used in the field component of Chami et al. [31]. For a description of the operating principle of the VSM, see Lee and Lewis [39].

The VSM measures the volume scattering function with 0.3 degree angular resolution from 0.4 – 178.5 degrees. We assumed that the volume scattering function was flat from 178.5 to 180 degrees, and then used a cubic interpolating spline to produce a VSF with 1-degree angular resolution from 0 to 180 degrees. We removed the volume scattering contribution by salt water according to Buiteveld et al. [27], and then estimated $b_{bp}(\lambda)$ according to Eq. (1) above.

After obtaining the particulate backscattering coefficient and volume scattering function from the VSM, we estimated $\chi_p(\lambda, \theta)$ by rearranging Eq. (2) as follows:

$$\chi_p(\lambda, \theta) = \frac{b_{bp}(\lambda)}{2\pi\beta_p(\lambda, \theta)} \quad (3)$$

We calculated $\chi_p(\lambda, \theta)$ at the six wavelengths of the VSM at one degree angular resolution from 90 to 180 degrees (Fig. 1, Table 2). We observed some minor spectral variability in the conversion factor between six wavelengths, but a one-way analysis of variance (ANOVA)

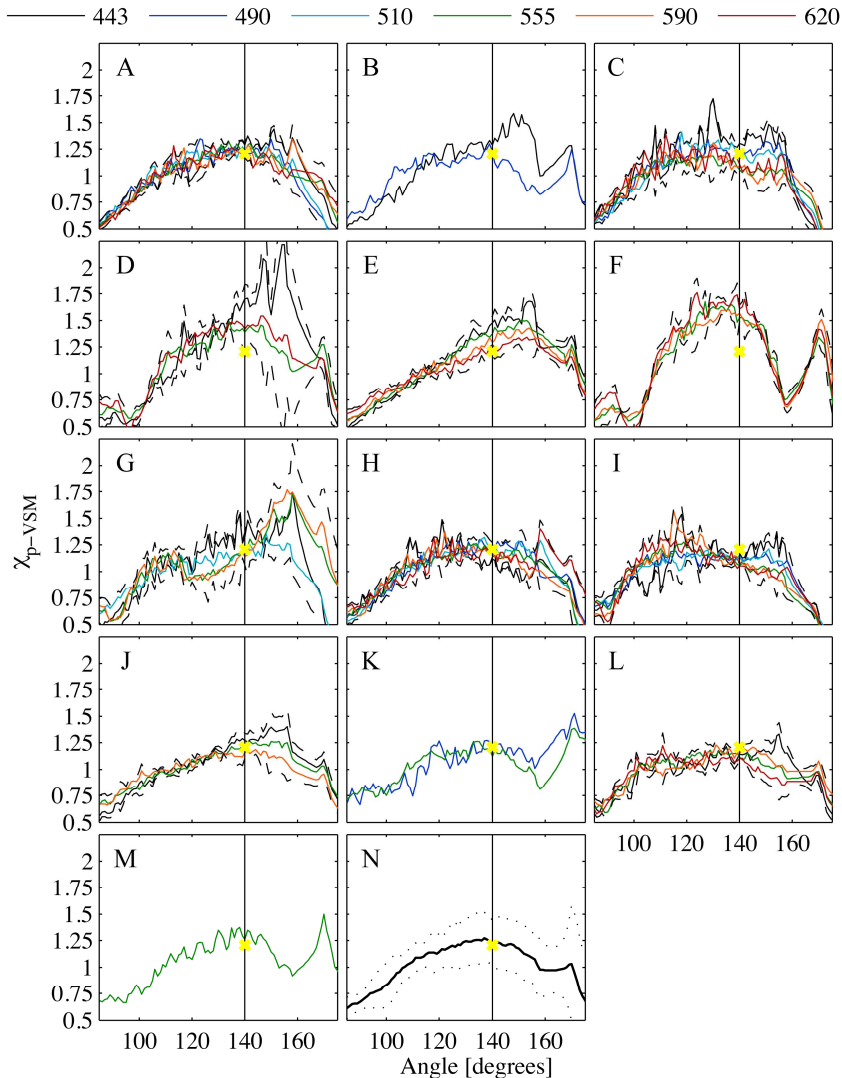


Fig. 1. Angular variation in χ_p for 13 phytoplankton cultures. The solid vertical line is the centroid measurement angle of the Hydrosat-6 (140°). A yellow 'X' is shown at $\chi_p = 1.21$, the mean value over all wavelengths and all cultures sampled. Where three or more wavelengths were used, dashed lines are shown at two standard deviations from the mean χ_p value for the culture. The measurement wavelengths (in nm) are shown in the legend above. The cultures shown are: (A) *Amphidinium carterae*, (B) *Ditylum brightwellii*, (C) *Dunaliella tertiolecta*, (D) *Emeliana huxleyi*, (E) *Gephyrocapsa oceanica*, (F) *Isochrysis galbana*, (G) *Prorocentrum minimum*, (H) *Pyramimonas parkeae*, (I) *Stephanopyxis turris*, (J) *Thalassiosphaera heimii*, (K) *Thalassiosira pseudonana*, (L) *Thalassiosira weissflogii*, (M) *Pycnococcus provasolii*, and (N) mean of all cultures at all wavelengths with 95% confidence intervals.

conducted on the means of all six wavelengths between 100 and 150 degrees found no significant difference between them ($P = 0.623$). We calculated relative standard deviation as a percentage of the mean value at each wavelength (or coefficient of variation times 100). It is interesting to note that the highest standard deviations were observed for the average $\chi_p(\lambda, 140)$ spectra that included data from more species, not fewer (e.g. 443, 555, 590 and 620 nm; see Table 2). This indicates that the width of the 95% confidence intervals shown in Fig. 2 are more indicative of the natural variability between species, rather than being a measure of uncertainty. $\chi_p(\lambda, \theta)$ shows the most variability at angles greater than 155 degrees, which may be the result of high variability in the near-backward scattering for various species, or reflections inside the VSM's sample chamber [39]. Our results closely followed the angular dependence observed in previous studies, showing a broad maximum in χ_p around 130 to 140 degrees (Fig. 2 [26,31];). Our results were generally consistent with estimates of χ_p at 555 nm for cultures published by Chami et al. [31] from 90 to 120 degrees, but were slightly lower from 130 to 160 degrees (nevertheless, still within the uncertainty of the VSM measurements). Our average estimates of χ_p for cultures most closely resembled those of Boss and Pegau [26] that were from data collected in the coastal waters of the Eastern United States with an earlier generation of the VSM, and Sullivan and Twardowski [34], who used another prototype scattering meter and analyzed data from a global set of VSF measurements.

Table 2. Average value and relative standard deviation, σ , of χ_p for thirteen phytoplankton species from 90 to 170 degrees at six wavelengths. N is the number of cultures available to calculate the mean and standard deviation

| | N | Measurement Angle [°] | | | | | | | | |
|---------------|-----|-----------------------|-------|-------|-------|-------|-------|-------|-------|-------|
| | | 90 | 100 | 110 | 120 | 130 | 140 | 150 | 160 | 170 |
| $\chi_p(443)$ | 10 | 0.64 | 0.85 | 1.01 | 1.13 | 1.28 | 1.30 | 1.35 | 1.16 | 0.90 |
| σ (%) | | 9.11 | 16.71 | 11.60 | 11.06 | 14.01 | 14.00 | 11.76 | 17.18 | 36.77 |
| $\chi_p(490)$ | 6 | 0.65 | 0.89 | 1.02 | 1.17 | 1.17 | 1.21 | 1.26 | 1.00 | 0.79 |
| σ (%) | | 4.36 | 8.37 | 15.39 | 5.12 | 7.22 | 3.83 | 5.87 | 9.91 | 53.54 |
| $\chi_p(510)$ | 5 | 0.65 | 0.89 | 1.01 | 1.23 | 1.18 | 1.21 | 1.23 | 1.03 | 0.77 |
| σ (%) | | 5.84 | 7.72 | 14.72 | 5.69 | 8.26 | 3.89 | 3.23 | 13.97 | 51.93 |
| $\chi_p(555)$ | 12 | 0.67 | 0.83 | 1.05 | 1.14 | 1.24 | 1.23 | 1.17 | 0.97 | 1.03 |
| σ (%) | | 7.90 | 14.89 | 7.81 | 9.42 | 10.64 | 11.12 | 12.87 | 14.77 | 32.38 |
| $\chi_p(590)$ | 9 | 0.63 | 0.86 | 1.10 | 1.14 | 1.20 | 1.22 | 1.22 | 1.08 | 0.96 |
| σ (%) | | 10.11 | 12.78 | 7.04 | 11.81 | 12.07 | 12.77 | 14.93 | 25.81 | 34.10 |
| $\chi_p(620)$ | 8 | 0.66 | 0.86 | 1.11 | 1.16 | 1.22 | 1.24 | 1.20 | 1.08 | 1.01 |
| σ (%) | | 12.32 | 22.86 | 12.31 | 13.13 | 15.98 | 13.39 | 15.20 | 23.59 | 32.55 |

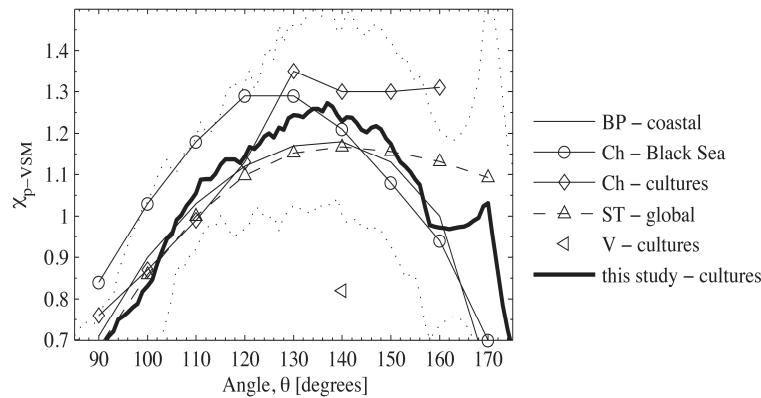


Fig. 2. Angular variation in mean χ_p for oceanic particles and phytoplankton cultures (see legend). χ_p at 555 nm is shown for this study (bold line) with 95% confidence intervals (dotted lines). The other wavelengths used were 532 nm for Boss and Pegau [BP; 26], 550 nm for Chami et al. [Ch; 31], 658 nm for Sullivan and Twardowski. [ST; 34], and 514 nm for Vaillancourt et al. [V; 21].

Contrary to Chami et al. [31], we found that χ_p was independent of wavelength at several angles within the uncertainty of our measurements (Fig. 1). As such, we calculated the average χ_p from all of the cultures at all wavelengths sampled in our study at 140 degrees and used the result, 1.21. We applied this single conversion factor on data collected for all cultures at all wavelengths when estimating the particulate backscattering coefficient with volume scattering data from the Hydrosat-6 instrument.

2.6 Optical cross-sections and efficiency factors

To facilitate comparisons of spectral shape and the efficiency of backscattering between cultures in a way that is independent of concentration, it is useful to normalize the backscattering measurements by some other variable. In the case of phytoplankton cultures, chlorophyll (chlorophyll-specific backscattering coefficient, b_{bp}^* ; Table 1), cell concentration, and particulate organic carbon content are commonly used (e.g. Vaillancourt et al. [21]). We normalized the particulate backscattering coefficient, and the other IOPs measured in this study, by cell concentration to produce IOP cross-sections for each culture. Single particle cross-sections, σ_x (where x is 'a' for absorption, 'b' for scattering, and 'bb' for backscattering), were calculated as the ratio of the bulk optical coefficient to particle concentration, N/V (particles per cubic meter), measured with the Coulter counter (or microscopy for larger species; see Table 1). For example, the backscattering cross-section, σ_{bb} , was estimated as follows:

$$\sigma_{bb} = \frac{b_{bp}(\lambda)}{N/V} \quad (4)$$

Particle optical cross-sections (units of m^2) describe the two-dimensional area of the particle that interacts with source light, and may or may not be directly related to the actual size or volume of the particle. For example, in the case of phytoplankton cells, pigment packaging may affect the absorption cross-section in a manner that is not linearly related to the cell size or volume [40]. Also, the scattering cross-section of a non-spherical cell may vary depending on the orientation of the cell relative to the source and detector.

A useful method for gauging the accuracy of the Coulter counter data is to calculate optical efficiency factors. Efficiency factors, Q_x (with the same subscript assignments as the cross-sections above), are the ratio of the optical (σ) and geometric (G) cross sections. The geometric cross section is the cross sectional area of the particle, which in this case is the area of a circle having the same diameter as the equivalent spherical diameter for each culture. For example, the backscattering efficiency factor, Q_{bb} , was estimated as follows:

$$Q_{bb} = \frac{\sigma_{bb}}{\pi \times r^2} \quad (5)$$

where r is the radius of the cells, computed as $1/2$ of the Coulter counter or microscope-based ESD. See Table 1 for the absorption, scattering, and backscattering efficiency factors at 442 nm.

2.7 Uncertainties in optical parameters

We estimated the standard deviations of the absorption, attenuation, and backscattering coefficients for all of the dilution series of all cultures (data collected for at least two minutes), and converted the data to the coefficient of variation (CV) to facilitate comparison between measurements at various concentrations. We found that for cultures, absorption measurements had an average (across all wavelengths) CV of approximately 1% of the signal. The attenuation measurement had an average CV of 0.5%. By propagation of error, the uncertainty in the scattering coefficient is 1.5%. Compared with Mie theory, Berthon et al. [32] estimated a 5% uncertainty in VSM measurements of the volume scattering function (at any given

angle) for spherical beads, and Boss and Pegau [26] estimated the uncertainty in χ_p at 140 degrees to be 3.5%. In our data, the average CV in χ_p at 140 degrees for cultures ranged from 3.8% - 14% depending on the measurement wavelength (Table 2). The average CV for χ_p at 140 degrees for all cultures across all wavelengths is 10%. The combined uncertainty due to measurement and natural variability in the conversion factor for cultures is estimated to be between 10 and 15%. The backscattering coefficient had an average CV of 3%. This reflects measurement uncertainty only. When combined with uncertainty in the conversion factor $\chi_p(\lambda, 140)$, we estimate the uncertainty in the backscattering coefficient to be around 15%. We estimate the uncertainty in the backscattering ratio to be approximately 15%. We did not collect replicate measurements of the particle counts from the Coulter counter, but we estimate the error in the mean particle size and concentration to be approximately 5%. We estimate the error in the absorption, scattering, and backscattering cross-sections as 6%, 5.5%, and 20% respectively.

3. Results

3.1 Spectral particulate backscattering coefficients

Particulate backscattering coefficients, $b_{bp}(\lambda)$, were obtained for each experimental culture using Eq. (2) (Fig. 3). Previous research has shown that measurements of backscattering at 676 nm can be artificially elevated due to fluorescence emission that is detected at this wavelength [17,41–43]. Our data corroborate these results and showed enhanced ‘backscattering’ at 676 nm for all cultures. We therefore excluded $b_{bp}(676)$ from our analyses,

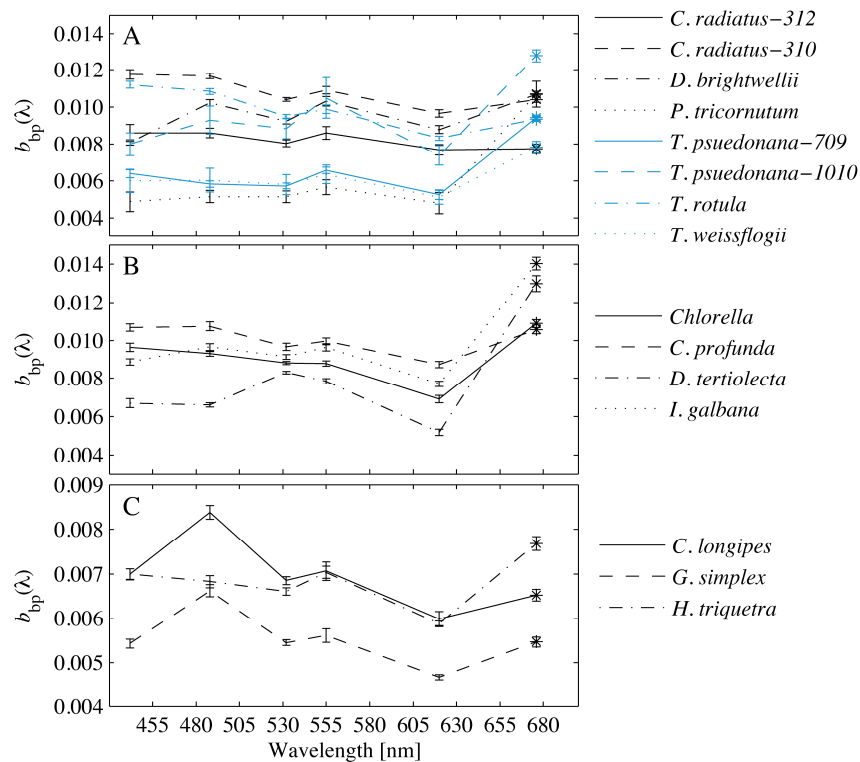


Fig. 3. Spectral backscattering coefficients for fifteen phytoplankton species. Error bars represent one standard deviation of the mean of data collected over at least two minutes. (A) Diatom species sampled. Where more than one strain was sampled, the strain number is shown. (B) Flagellates. (C) Dinoflagellates. Data shown at 676 nm are contaminated by fluorescence (denoted with an asterisk). These data are shown for reference only.

but show the data in the figures for reference (Fig. 3,4). The shape of the particulate backscattering coefficient spectra for phytoplankton cultures showed distinct features within and between taxonomic groups. Backscattering generally decreased from blue to red with the exception of backscattering at 442 nm, where pigment absorption has been shown to influence backscattering intensity [17,19].

For non-absorbing particles, Mie theory predicts that particles with a high scattering cross section (large particles) will have similar backscattering at all wavelengths, whereas smaller particles will have relatively higher backscattering at shorter wavelengths [44,45]. As a result, smaller cells would produce a sloped spectrum, and larger cells a relatively flat spectrum. This size/spectrum relationship is of particular interest in ocean color remote sensing, where the inversion of spectral ocean color to spectral backscattering could provide information regarding bulk particle size (e.g [46]). We calculated the ratio of backscattering at 488 nm to 620 nm as a general indicator of the slope of the backscattering spectrum. We did not find a significant relationship between the equivalent spherical diameter of phytoplankton cells and ratios of the backscattering coefficient at different wavelengths in our data set (not shown).

3.3 Spectral particulate backscattering ratios

The particulate backscattering ratios of the marine phytoplankton cultures that we sampled ranged from 0.0035 – 0.0290 at 442 nm (see Table 1; Fig. 4). Although there is some apparent

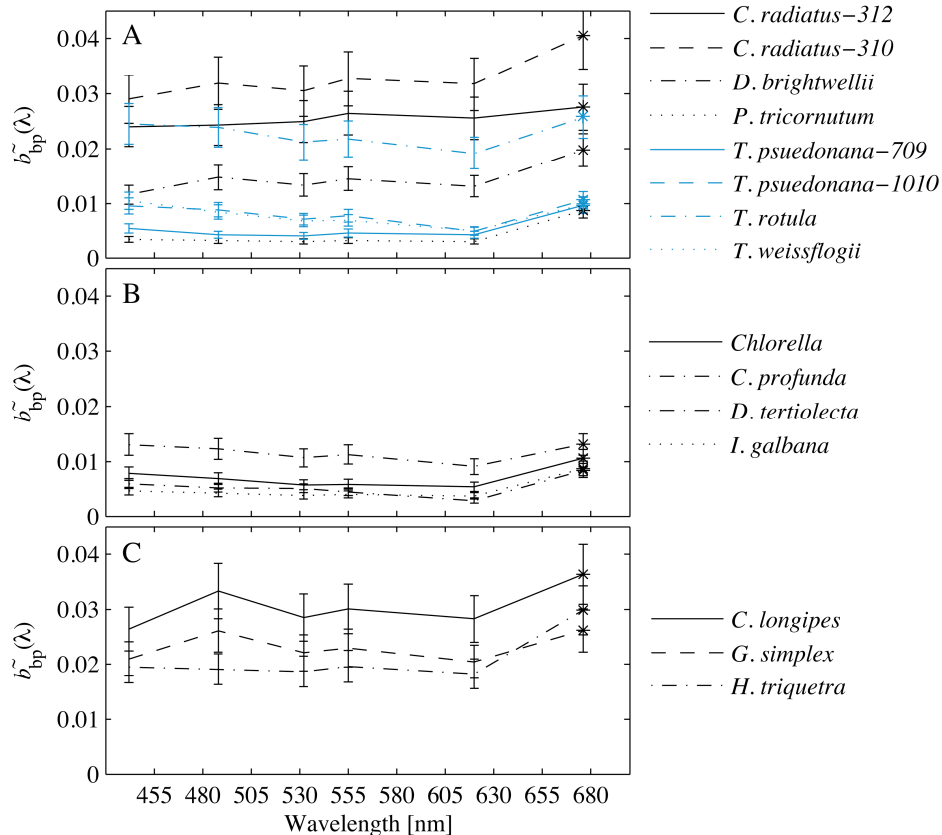


Fig. 4. Spectral particulate backscattering ratios for fifteen phytoplankton cultures, separated into taxonomic groups. Error bars show 15% of the signal at each wavelength. (A) Diatoms. Where more than one species was sampled, the strain number is shown (B) Flagellates (C) Dinoflagellates. Data shown at 676 nm are contaminated by fluorescence (denoted with an asterisk). These data are shown for reference only.

spectral variability, the differences between wavelengths for individual taxa were mostly within the 15% error in our estimates (Fig. 4). Cultures with the lowest backscattering ratios, from 0.0035 to 0.0131, included *C. profunda*, *Chlorella sp.*, *D. tertiolecta*, the prymnesiophyte *I. Galbana*, small centric diatoms (both strains of *T. pseudonana*, and *T. weissflogii*), a large centric diatom (*D. brightwellii*), and the pennate diatom *P. tricorutum* (Fig. 4). The highest backscattering ratios, from 0.0195 to 0.0290, were observed in large centric diatoms (both strains of *C. radiatus*, and *T. rotula*) and all of the dinoflagellates sampled (*C. longipes*, *G. simplex*, and *H. triquetra*). This result illustrates that the backscattering ratios in marine phytoplankton cultures are not simply the result of plasma membrane and cell wall material [47] (i.e. silica vs. cellulose thecal plates), but are instead the result of complex interactions with size, shape, and the internal structures of the cells.

Except for the cryptophyte *C. profunda*, the remaining flagellates sampled, *I. galbana*, *Chlorella sp.*, and *D. tertiolecta*, all had backscattering ratios of 0.0079 or less. Based on modeling studies that assumed homogeneous spherical particles, Morel and Ahn [15] concluded that heterotrophic flagellates and ciliates had almost no effect on backscattering. Our measurements support their results to the extent that the autotrophic flagellates sampled in this work produced weak, but not insignificant, backscattering. The weak backscattering in these groups can be attributed to their relatively high water content [15].

3.4 Backscattering and chlorophyll

When data from all cultures was grouped together, high backscattering values were observed at low, intermediate, and high chlorophyll concentrations, indicating that chlorophyll concentration was not a good predictor of backscattering, and vice versa, for phytoplankton cultures in toto [Fig. 5(A)]. However, for each species in our study, backscattering was linearly correlated with the chlorophyll concentration when examined individually [Fig. 5(B), 5(C)]. The slope of the relationship was species-specific. For example, *T. pseudonana* (CCMP1010) had a chlorophyll-*a* concentration of nearly 20 mg m⁻³ with a concurrent backscattering coefficient at 555 nm of 0.011 m⁻¹, whereas *C. longipes* had a chlorophyll-*a* concentration of only 0.75 mg m⁻³ at a $b_{bp}(555)$ of 0.008 m⁻¹. This observation helps to explain the wide range of variability that we observe between chlorophyll-*a* and backscattering in situ, where individual members of the phytoplankton community variously contribute to the bulk signals. This result also provides some explanation as to why the b_{bp} :chlorophyll *a* ratio can exhibit up to 30% variability, even in case-1 waters [43]. Such variability is not necessarily the result of flaws in our assumptions about the nature of case-1 waters, measurement error, or the varying presence of non-algal particles (detritus, lithogenic material, non-photosynthetic bacteria, etc.). Although the relationship between b_{bp} and chlorophyll *a* has been shown to be highly linear in case-1 waters [43,48], the variability around this relationship could be explained more mechanistically as natural variability due to mixed phytoplankton populations, as well as photoadaptation that alters the chlorophyll to carbon ratio.

4. Discussion

4.1 Variability in the spectral particulate backscattering coefficient

We observed spectral variability in the backscattering coefficients of marine phytoplankton cultures that we could not attribute to cell size or absorption effects. Likewise, there were no obvious correlations between features in the attenuation, scattering, or absorption spectra and spectral variability in the backscattering coefficients of the cultures. It is possible that the limited number of usable wavelengths (five) and wide spectral bands (10 nm FWHM) of the Hydrosat-6 instrument were insufficient for examining the spectral features seen in previous work [12,17,19]. However, given the lack of published direct measurements of the backscattering properties of marine phytoplankton cultures, more general information on the

backscattering properties of marine phytoplankton cultures is still needed. Despite the lack of strong spectral features in the backscattering coefficients, we did not fit a power law function

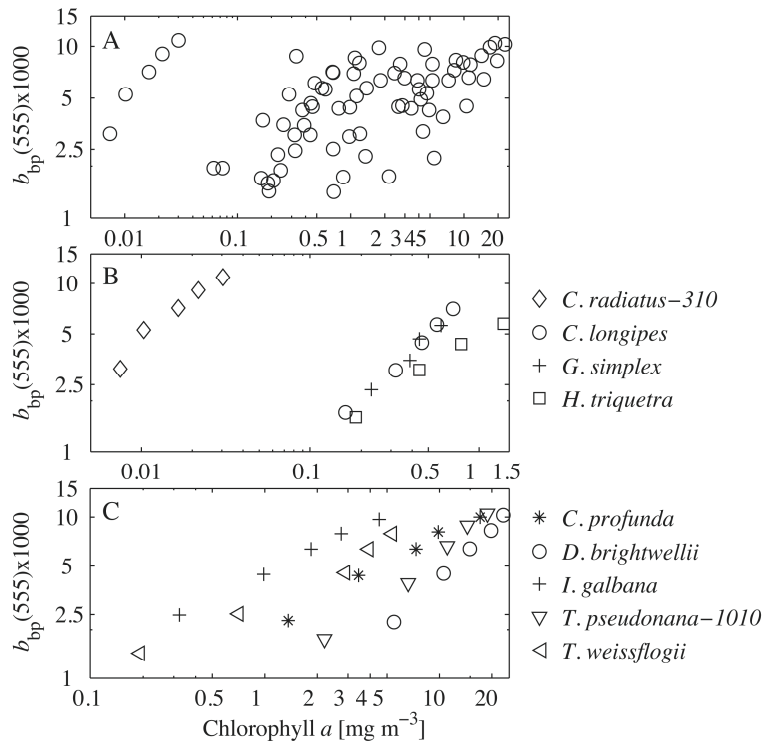


Fig. 5. The backscattering coefficient at 555 nm $\times 1000$ versus chlorophyll- a concentration for culture dilution series experiments. (A) data for all cultures (B) data for selected cultures with chlorophyll concentrations of less than 1.5 mg m^{-3} (C) data for selected cultures with chlorophyll- a concentrations up to 25 mg m^{-3} .

to the spectra in an effort to produce ‘representative’ phytoplankton spectra as in previous studies [21]. There is no evidence to support the idea that individual phytoplankton cells or nearly monodispersed cultures would adhere to such a generalized spectral shape, especially given the extremely variable nature of phytoplankton size, morphology, and composition. Stramski et al. [19], who presented the collected results of eight published papers on phytoplankton optical properties (though backscattering results were all derived from models), demonstrated that there was extreme spectral variation in the modeled particulate backscattering coefficients between species and phytoplankton groups that our measurements could not replicate. While our observations indicated that spectral backscattering differences were not influenced by particle size or shape, the magnitude backscattering ratio, in contrast, was quite sensitive to particle composition. We discuss these results in the next section.

We also investigated the influence of absorption on the backscattering signal at 442 nm to determine if strong chlorophyll absorption diminished backscattering [12,17]. We estimated the slope of the backscattering spectrum between 442 nm and 488 nm, and compared these slopes to the absorption line height at 442 nm (e.g [41,49]). We did not find any significant relationship between the absorption line height and the slope of the backscattering spectrum between 442 nm and 488 nm when all cultures were combined. However, when we considered each taxonomic group individually, the slope of the backscattering spectrum in the blue for flagellates and dinoflagellates showed a strong relationship with the absorption line height when the data were fit with linear least squares regressions [$R^2 = 0.93$ and 0.99].

respectively; (see Fig. 3.6 in [50]). Flagellates exhibited a positive slope at high absorption, i.e. $b_{bp}(442)$ was lower than $b_{bp}(488)$. The dinoflagellates demonstrated the opposite trend, with high, positive backscattering slopes at low values of the absorption line height, and a negative slope at higher line height. The slopes of the backscattering spectra between 442 nm and 488 nm for the diatoms had a weaker, positive linear relationship with the absorption line height ($R^2 = 0.25$). It is not clear at this time why absorption had such a variable effect on the observed magnitude of backscattering between cultures. It is likely that the wide angular and spectral ranges of the HS6 detectors (25° and 10 nm FWHM respectively), acted to integrate and diffuse the depressive effect of absorption (10 nm FWHM), which is known to occur over a relatively narrow spectral range [see 18,19], making the effect difficult to observe directly.

4.2 Variability in the spectral particulate backscattering ratio between cultures, and comparison with previous models

Backscattering ratios for the diatoms that we sampled were highly variable, spanning nearly an order of magnitude from the highest observed to the lowest (0.0035 to 0.0290; Table 1). Given the range in size and variety of shapes for the eight diatoms that we sampled, the backscattering ratio appears to be largely a function of size for this group. In general, the larger diatoms exhibited higher backscattering ratios and larger backscattering cross-sections than smaller diatoms. The presence of spines (*D. brightwellii*) did not appear to have a significant effect on the backscattering ratio in these cultures.

The dinoflagellates, which range in size from just under 12 μm to over 150 μm in our cultures, all had very high backscattering ratios (Table 1). This was consistent for both thecate (having cellulose thecal plates embedded in the cell membrane, *H. triquetra*) and non-thecate (lacking thecal plates, *G. simplex*) dinoflagellates. This supports the idea that cell composition and internal structure play a large role in backscattering [7,12,20,51]. Vaillancourt et al. [21] also found that dinoflagellates had the highest backscattering efficiency out of 12 classes of phytoplankton, which they attributed to the high relative carbon content of the group (carbon content per cell volume).

In addition to their high carbon content, dinoflagellates also have some unique internal structures that may contribute to increased backscattering. First, they have an organelle called a pusule, which is described as “an array of highly branched membranous sacs or tubules derived by invagination of the cell membrane” [52]. These organelles are generally found in association with the flagella, and may be 2 to 10 microns in diameter (with much higher surface area due to their complex structure). The cell membrane of an algal cell is primarily lipids and proteins, and can have a refractive index as high as 1.10-1.16 relative to water [5]. If we assume the pusules maintain the same index of refraction as the cell membrane, they could significantly influence the backscattering properties of the cells by increasing the structural complexity and surface area of highly refractive material within the cells. Theoretically, this would result in high backscattering cross-sections (σ_{bb}) relative to other phytoplankton groups with cells of the same size. While our sample size is small, *G. simplex* and *H. triquetra* do have higher σ_{bb} than comparably sized diatoms *T. pseudonana* (CCMP1010) and *T. weissflogii* (Table 1).

Dinoflagellates also have very unusual chromosome morphology that is unique among eukaryotes [53]. The chromatin of dinoflagellate deoxyribonucleic acid (DNA) lacks histones and nucleosomes, which results in chromosomes that remain permanently compressed except during DNA replication [53]. Their chromosomes stay in very dense clusters in the nucleus, and contain large amounts of DNA. Their protein:DNA mass ratio is 1:10, whereas normal eukaryotes have a 1:1 ratio [53]. The refractive index of DNA is 1.16 (relative to water) at 632 nm [54], which is significantly higher than reported values for surrounding cytoplasm. Kitchen and Zaneveld [7] showed that the backscattering from a three-layered-sphere model of a phytoplankton cell was more than an order of magnitude higher than for the same size homogeneous sphere. However, Kitchen and Zaneveld [7] used an index of refraction of only

1.02 for the inner layer of the model sphere. A model representing the dense aggregation of high refractive index DNA within the dinoflagellate nucleus would produce backscattering coefficients that were even higher than the ten-fold increase observed in Kitchen and Zaneveld's hypothetical phytoplankton cell. It is possible that the unique nucleus of the dinoflagellates could alone explain the high backscattering ratios that we observed, regardless of the possible contribution of the pusules.

The sole cryptophyte in our study, *C. profunda*, exhibited a relatively high backscattering ratio of 0.0131 at 442 nm. We hypothesize that the ratio was influenced by the unique plated periplast found in cryptomonads [55,56]). The periplast is a three-layer cell membrane that is composed of an internal plasma membrane, an inner layer proteinaceous plates, and an outer fibrous layer. We speculate that the protein content of the periplast acts as a high refractive index outer shell, the effect of which has been shown to significantly increase backscattering in several studies [5–7,57]. The backscattering ratio for *C. profunda* was higher than that of a comparably sized diatom, *T. weissflogii*, which suggests that the cell covering may be responsible for the high backscattering efficiency observed in this culture.

We also found that the backscattering ratio was weakly influenced by cell size [Fig. 6(A)]. We fit a power law function to the backscattering ratio at 555 nm and the equivalent spherical diameter (ESD) and found that the relationship was described by the following function:

$$b_{bp} / b_p (555) = 4.390 \times 10^{-3} \times \text{ESD}^{0.432}; R^2 = 0.56 \quad (6)$$

A similar relationship was observed between the backscattering cross-section at 555 nm and the ESD:

$$\sigma_{bb} (555) = 4.269 \times 10^{-14} \times \text{ESD}^{2.028}; R^2 = 0.84 \quad (7)$$

These results are somewhat counter-intuitive for the backscattering ratio because, all else being equal, a larger homogeneous particle has a lower backscattering efficiency than a smaller homogeneous particle. This is because larger particles scatter more light in the forward direction than smaller particles, which reduces their backscattering ratio. It is not surprising however, that the optical cross-section, σ_{bb} , exhibits a stronger relationship (higher R^2) with the geometric cross-section (size, ESD^2). This is generally true for particles with a diameter that is much greater than the wavelength of incident light [9]. Vaillancourt et al. [21] also found a strong positive relationship between backscattering efficiency and cell diameter. One possible explanation of the relationship between the backscattering ratio and ESD is that the cultures of larger cells had high concentrations of detrital material or bacterial contamination, and that these small, non-algal particles elevated the backscattering magnitudes of the larger cells. However, given the difficulty of differentiating the potential effects of these non-algal particles from the signals originating from the cells of interest, we were unable to quantify their possible influence on our results (see Section 4.4 for an examination of this issue). Another explanation may be that the larger the cell, the smaller the

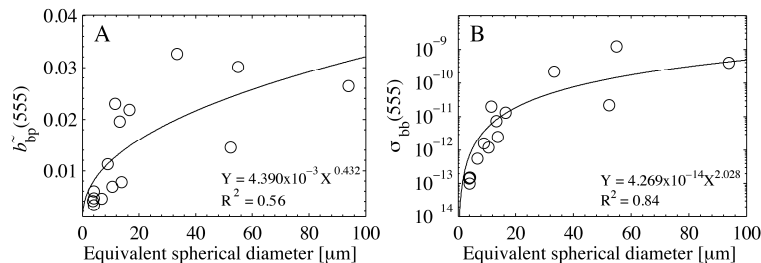


Fig. 6. (A) The particulate backscattering ratio at 555 nm versus the equivalent spherical diameter for phytoplankton cultures measured with a Coulter counter or light microscopy. (B) The backscattering cross-section at 555 nm versus the equivalent spherical diameter for phytoplankton cultures. The equations for a power law fit and the R^2 of the fits are shown.

ratio of surface area to volume. Increasing size decreases the cell wall contribution to the optical signal (for cells of similar composition). This explanation would imply that the complex internal structure of phytoplankton cells is a mechanism for increased backscattering signal relative to a homogeneous sphere model, and that the effect of internal structure would dominate the effect of a high refractive index cell wall, which contradicts our interpretations for high backscattering ratios observed in dinoflagellates and cryptomonads. A final explanation for the positive relationship between cell size and backscattering ratio may be that the complex composition and internal structure of phytoplankton cells trump simplistic model interpretations of the way that light interacts with these particles. Our a priori assumption that “all else is equal” between two phytoplankton cells, aside from their size, may not apply to interpretations of their backscattering properties.

4.3 Comparison to other measured and modeled values of phytoplankton IOPs

Optical cross-sections are a useful parameter for comparing the spectral optical properties of phytoplankton cells because the effect of concentration is removed and spectral shape can be examined. We found that the backscattering cross section ranged from $8.60 \times 10^{-14} \text{ m}^2 \text{ cell}^{-1}$ to $1.23 \times 10^{-9} \text{ m}^2 \text{ cell}^{-1}$ at 442 nm (Table 1). We compared our results with the most recently published review on the inherent optical properties of phytoplankton cells [19], and found agreement between absorption and scattering cross-sections [Fig. 7(A), 7(B)]. In contrast, for the backscattering cross-section and backscattering ratio, we observed values up to one and two orders of magnitude higher, respectively, than previous work [19] [Fig. 7(C), 7(D)]. However:

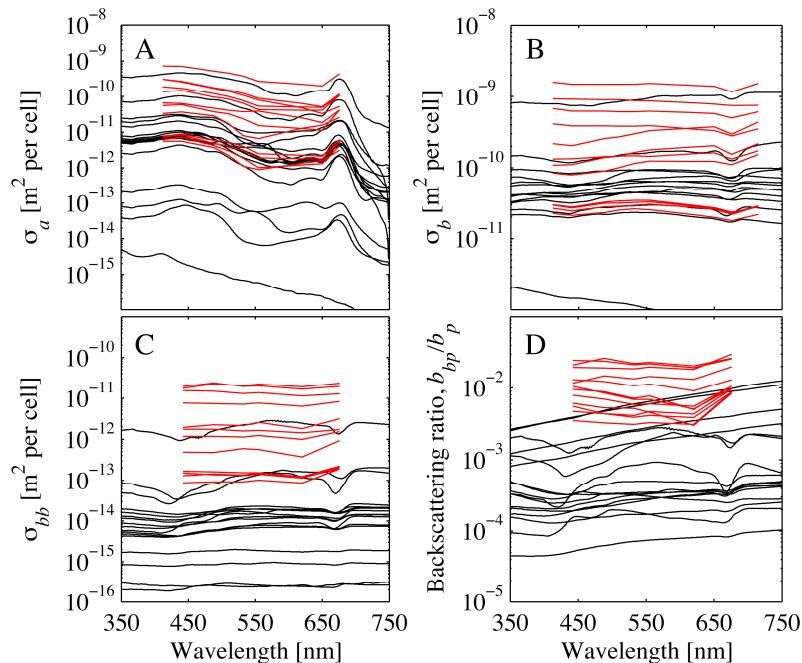


Fig. 7. Spectral values of IOP cross-sections and backscattering ratios for cultures that were in the same size range as those shown by Stramski et. al. (2001). Red lines are our data, black lines are from Stramski et. al. (2001). The absorption (A) and scattering cross-sections (B) from Stramski et. al. (2001) were based on measurements. The backscattering cross-section (C) and backscattering ratio (D) were model results in Stramski et al. (2001), and were measured in our study.

these discrepancies between the backscattering magnitudes were not unexpected. The backscattering data from Stramski et al. [19] were model results, and as discussed previously, the Mie model is likely to severely underestimate backscattering for non-spherical particles [8,9]. It is also likely that the inhomogeneity of phytoplankton cells (i.e. the presence of cell walls and organelles) increases backscattering more than can be explained by the most commonly used models [5–7,20]. The same rationale can be used to explain the higher backscattering ratios in our results compared to previous model results (Fig. 7(D) [57];).

4.4 Presence of unspecified non-algal particles

Non-phytoplankton particles are an unavoidable component of most laboratory cultures. Phytoplankton ‘monocultures’ are often a combination of the target culture, resident heterotrophic bacteria, organic, non-living particles composed of dead cells or sloughed cell fragments, and various flocs containing all of the above. These non-target particles pose a considerable problem when trying to characterize the optical properties of phytoplankton cells. We tried to address this concern in our sampling methods by filtering all culture media through a 0.2 μm filter prior to sampling, and by sampling when the cultures were in exponential growth (which tend to have lower bacterial populations and other particulate material compared to cultures in stationary phase). However, we acknowledge that completely avoiding the presence of non-algal particles in cultures is impossible. The presence of small, non-algal particles (including bacteria and detritus, hereafter called simply NAP) was indicated in the Coulter counter data of eight of fifteen cultures as higher than background particle counts in the lowest few size bins. A high signal in the lowest size bins potentially indicates the presence of bacteria or other NAP that could significantly influence the measured optical properties of the cultures. However, it has also been shown that data collected in the smallest size bins of the Coulter counter are biased by noise and may not be usable [58]. It is also possible that the presence of flocculated detrital material was transformed by aperture shear disaggregation into small particles that were not actually present in the sample chamber.

The backscattering coefficient, b_{bp} , is especially sensitive to this kind of contamination because of the high backscattering efficiency of small particles (based on Mie theory; <3 microns [16];). However, backscattering data alone were not sufficient to indicate contamination in our cultures because a high backscattering signal was also observed on non-indicated cultures. The fact that for most cultures the values for the optical efficiency factors computed using the phytoplankton cell counts were consistent with theory ($Q_a < 1$, $Q_c < 4$), suggests that contamination was relatively low. If contamination by small particles was high, the cell count data and microscopy would have provided too-small a geometric cross-section resulting in overestimated efficiency factors (as observed, e.g., for *Coscinodiscus radiatus-310*). Of the fifteen cultures sampled, four had efficiency factors that indicated that particles other than the target culture were likely to be contributing to the optical signals (Table 1). While these cultures did have among the highest backscattering ratios (also a possible indication of contamination by small particles), there were two cultures with reasonable efficiency factors that also had high backscattering ratios (*Ceratium longipes* and the larger *Coscinodiscus radiatus* strain). For the eleven cultures with reasonable efficiency factors, the range in values agrees well with Q_{bb} data shown in Vaillancourt et al. [21]. Our observations indicate that achieving a “pure culture” and distinguishing the phytoplankton signal from non-algal particles in culture is probably our greatest challenge in determining the optical properties of marine phytoplankton on a per-cell or per-species basis. Despite this, we believe that our measurements reflect the actual backscattering properties of the phytoplankton cells studied in this work, with the caveat that the NAP associated with these cells may have provided some unknown (and perhaps significant) portion of the signals.

5. Conclusions

The objective of this study was to examine the contribution of phytoplankton size, shape, and morphology to variability in backscattering. To this end we measured the VSF and the absorption and attenuation coefficients at several wavelengths for thirteen phytoplankton species (a total of fifteen strains). We also collected samples for chlorophyll-*a* concentration, and for cell counts and sizing via microscopy and Coulter counter. Despite the fact that we took measurements at just six wavelengths, we were able to detect differences in the backscattering properties of the cultures, and relate these properties to differences in cellular structure and composition. We found that the spectral backscattering properties of phytoplankton deviate from theory at wavelengths where pigment absorption is significant. We were not able to detect an effect of cell size on the spectral shape of backscattering, but did find a relationship between cell size and both the backscattering ratio and backscattering cross-section. Results also indicated that while particulate backscattering at 555 nm was well correlated to chlorophyll-*a* concentration for any given species, the relationship was highly variable between species. This helps to explain why chlorophyll-*a* concentration is not a universal predictor of the magnitude of backscattering in situ.

The most significant finding in this work was that phytoplankton cells may be a source of significant backscattering, in contrast to model predictions that are unable to account for the complex internal structure and morphology of phytoplankton cells, or their various cell coverings. There is a longstanding, unresolved mystery among bio-optical oceanographers referred to as the “backscattering enigma” [4]. In making budgets for light scattering in the open ocean in non-bloom conditions, previous estimates were unable to account for a large portion of backscattered light. I.e., more light was backscattered from the ocean surface up to remote sensors than could be accounted for in theoretical models [15,16]. Many researchers invoked the presence of small detrital particles that could not be physically discriminated from other oceanic particles as the source of the “missing backscattering” [15,16,44]. Model efforts using non-spherical particles [9] or layered spheres [7] have provided some basis for the argument that phytoplankton cells could realistically be a source of higher backscattering than previously thought, but the paucity of measurements of phytoplankton backscattering had left the “enigma” as an open question. Our results, some of the first of their kind, demonstrate that phytoplankton cells may have significant backscattering efficiencies, likely owing to their complex cellular compositions and morphologies. This finding suggests that we may no longer have to make the assumption that very small particles (in this work, greater than 0.2 μm and less than 1 μm), that we can’t detect or measure specifically, must be present in order to close a backscattering budget for particles in the ocean. Recent in situ measurements also support this conclusion [43]. Our results also suggest that further studies on the scattering properties of phytoplankton cultures are necessary. Measurements of the full volume scattering function of phytoplankton cultures, bacteria, and detritus (if possible) are necessary to better understand which aspects of phytoplankton cells (cell wall material and thickness, shape, etc.) are responsible for the differences in their backscattering properties.

Acknowledgments

The authors are deeply indebted to the diligent and careful laboratory work of Amanda Ashe, Chad Waluk, Laura Azevedo, and Iain MacCallum. We thank Michael Lee, Oleg Martynov, and Eugeny Shybanov from the Marine Hydrophysical Institute, National Academy of Science of Ukraine for sharing the volume scattering meter data with us, and Jennifer Prentice (formerly with NAVAIR) for organizing the Scattering Workshop where the data were collected. We appreciate Dariusz Stramski’s generosity in sharing his database on phytoplankton optical properties with us. We appreciate thoughtful comments from three reviewers, which helped to improve an earlier version of this manuscript. This work was funded by the National Aeronautics and Space Administration (NASA) grant NAG5-12393 to

L.K.-B. Funding support for A. Whitmire was provided by the American Society for Engineering Education, National Defense Science and Engineering Graduate Fellowship Program during the data collection and analysis phase of this work, and by the Agouron Institute (Grant AI-MME1.05) during the publication phase. E.B.'s work on IOPs has been supported by the Environmental Optics program of ONR.